

Original Research

Study and Characterization of a Spherical Solar Collector. Part II: Comparative Analysis with Flat-Plate Devices

Carlos Armenta-Déu *

Renewable Energy Group, Faculty of Physics, Complutense University of Madrid, 28040 Madrid, Spain; E-Mail: cardeu@fis.ucm.es* **Correspondence:** Carlos Armenta-Déu; E-Mail: cardeu@fis.ucm.es**Academic Editor:** Mariano Alarcón**Special Issue:** [Solar Thermal Energy](#)*Journal of Energy and Power Technology*
2023, volume 5, issue 3
doi:10.21926/jept.2303025**Received:** May 18, 2023**Accepted:** July 24, 2023**Published:** July 27, 2023

Abstract

The paper analyses the performance of a spherical solar collector compared to the efficiency of a flat-plate solar collector, which is the type of solar collector that does not use a tracking system in collecting solar radiation for energy conversion. Spherical solar collector benefits from a constant value of the angle of incidence, which optimizes the solar radiation that strikes the absorber of the solar device and maximizes the energy collection. Besides, the spherical geometry has a larger area for equal dimensions, width, and length. The combined effect of a larger surface and a higher value of the effective solar radiation onto the surface of the absorber increases the energy collection and the performance of the solar device. We developed a theoretical analysis to obtain the algorithm to determine the collected solar energy, which increases when using the spherical solar collector. A simulation runs to calculate the predicted values. We developed experimental tests in a spherical solar collector of 1.05 m in diameter, and in a flat-plate solar collector of 1.94 m × 1.025 m. to validate the simulation. The comparative analysis shows that a spherical solar collector generates more energy than a flat-plate one of the same absorbing surface by a factor of 2.09, and 7.75 times more if the width and height of the flat-plate collector equals the diameter of the spherical one.



© 2023 by the author. This is an open access article distributed under the conditions of the [Creative Commons by Attribution License](#), which permits unrestricted use, distribution, and reproduction in any medium or format, provided the original work is correctly cited.

Keywords

Spherical and flat-plate solar collector; comparative analysis; collected solar energy increase

1. Introduction

Flat-plate solar collectors are the most widely used devices for low-temperature applications. The low operating temperature of this kind of device limits the number of applications for solar cooking, water and air heating, and agricultural produce drying processes [1].

Spherical solar collectors are not equipped with a solar tracking system [2], and currently do not have a concentration effect [3]; however, they operate all day long without a tracking system. On the other hand, the symmetric distribution of the absorber area related to the incident solar radiation optimizes the energy collection [4-6]. Spherical solar collectors, however, suffer from higher energy losses due to the shadow area of the absorber surface [7]. To avoid thermal losses from this section, we cover the non-illuminated area with a thermal insulation film that prevents infrared radiation.

Spherical solar collectors show advantages and drawbacks in operating performance compared to flat-plate collectors [8, 9]; therefore, it is necessary to develop a detailed study to determine the suitability of using spherical solar collectors instead of flat-plate ones in low-temperature applications.

Many studies are devoted to the performance analysis of spherical solar collectors, some of them already mentioned in the previous paragraphs. Other works deal with the type of absorber [10, 11], the geometry of the design [12, 13], the kind of application, water heating [14-16] or heating and cooling [17], the structure and characteristics of the storage system [18], or the improvement of the collector's performance [19].

Other texts work on variations of the spherical geometry like semi-spherical collectors, which are similar in structure and characteristics with the difference of having only half of the geometrical development; among them, we can mention those devoted to the performance analysis [20], the evaluation of the received solar energy [21], the surface thermal distribution [22], or the analysis of heat losses [23].

Specific work studies the performance of solar air heaters (SAH), either using a triangular surface configuration [24], modifying the surface structure to simulate the SAH performance [25] or improving heat transfer [26], or evaluating the influence of a single and double-pass in SAH with thermal storage [27]. Finally, other texts analyze the environmental impact of SAH [28].

Despite all the previously developed work, the paper represents an advanced study on the comparative performance of spherical solar collectors related to the conventional flat-plate ones due to the specific treatment of the incoming solar radiation into the daily collected energy, considering the contribution of direct and diffuse solar radiation separately, and the influence of the angle of incidence of each component.

2. Theoretical Background

Collected solar energy by a solar collector depends on the solar radiation intensity that arrives at the solar collector absorber and the effective area of the absorber.

Solar radiation intensity arriving at the solar collector absorber depends on the angle of incidence through a coefficient known as Incidence Angle Modifier (IAM). The expression that determines the Incidence Angle Modifier is [29]:

$$K_{\tau\alpha}(\tau\alpha) = (\tau\alpha)/(\tau\alpha)_n = 1 - b_o(1/\cos\theta - 1) \quad (1)$$

The coefficient $(\tau\alpha)$ is the optical efficiency of the solar collector, which considers the transmission factor of the cover (τ) and the absorption coefficient of the solar collector absorber (α). Sub-index n in equation 1 indicates perpendicular incidence, and θ represents the solar radiation angle of incidence. The coefficient b_o depends on the solar collector's structure. The current value for a standard flat-plate solar collector with a single glass cover is $b_o = 0.1$ [30].

The expression for the angle of incidence of solar radiation is (Equation 2) [31]:

$$\begin{aligned} \cos\theta = & \sin\delta\sin\phi\cos\beta - \sin\delta\cos\phi\sin\beta\cos\gamma + \\ & + \cos\delta\cos\phi\cos\beta\cos\omega + \cos\delta\sin\phi\sin\beta\cos\gamma\cos\omega + \\ & + \cos\delta\sin\beta\sin\gamma\sin\omega \end{aligned} \quad (2)$$

The parameters δ , ϕ , β , γ , and ω account for declination, latitude, tilt of the solar collector, azimuth, and solar hourly angle, respectively.

The solar radiation intensity depends on the IAM factor:

$$G_{eff} = G_o K_{\tau\alpha}(\tau\alpha) \quad (3)$$

Although equation 1 is only valid for direct radiation, we can apply it to global radiation if we consider hemispheric diffuse radiation as a kind of "direct radiation" coming from a specific direction [32]. In the case of the isotropic atmosphere, the direction matches an incidence angle of 60° [33], and equation 3 transforms in:

$$G_{eff} = BK_b(\tau\alpha) + DK_d(\tau\alpha) \quad (4)$$

Where B and D represent the direct and diffuse solar radiation, and $K_b(\tau\alpha)$ and $K_d(\tau\alpha)$ are the IAM coefficients for direct and diffuse components of the solar radiation.

Combining equations 1 and 4:

$$G_{eff} = B[1 - b_o(1/\cos\theta - 1)] + D[1 - b_o] \quad (5)$$

If we use global radiation:

$$\theta = \tan^{-1}\left(\frac{W}{D}\right) + \frac{1}{2}\tan^{-1}\left(\frac{d - W}{D}\right) \quad (6)$$

W is the surface width, d is the Sun diameter, and D is the Earth to Sun distance.

Since $W \ll d$ and $W \ll D$, equation 6 transforms in:

$$\theta = \frac{1}{2} \tan^{-1} \left(\frac{d}{D} \right) = \frac{1}{2} \tan^{-1} \left(\frac{1.39 \cdot 10^9}{1.495 \cdot 10^{11}} \right) = 0.27^\circ \quad (7)$$

Equation 4 gives the instantaneous value of the effective solar radiation; however, it is more practical to use the daily average value, which we obtain from the equation [34]:

$$\bar{G} = \bar{B}r_b + \bar{D}r_d \quad (8)$$

\bar{B} and \bar{D} are the daily average values of direct and diffuse components of solar radiation. Coefficients r_b and r_d represent the ratio of collectible energy of a spherical to flat plate collector for direct and diffuse radiation; we obtain the coefficients from the equations [34]:

$$r_b = \frac{\bar{B}S_{sph}\Delta t_b \frac{t_{ss} - t_{sr}}{\Delta t_b}}{\bar{B}S_{FP}\Delta t_b} = \left(\frac{12}{\pi} \theta \right)^2 \frac{t_{ss} - t_{sr}}{\Delta t_b} = \left(\frac{12}{\pi} \theta \right)^2 \frac{L_d}{\Delta t_b} \quad (9)$$

$$r_d = \frac{(\bar{G} - \bar{B})S_{sph}(t_{ss} - t_{sr})}{(\bar{G} - \bar{B})S_{FP}(t_{ss} - t_{sr} - \frac{12}{\pi} \beta)} = \left(\frac{12}{\pi} \theta \right)^2 \frac{t_{ss} - t_{sr}}{(t_{ss} - t_{sr} - \frac{12}{\pi} \beta)} = \left(\frac{12}{\pi} \theta \right)^2 \frac{L_d}{(L_d - \frac{12}{\pi} \beta)} \quad (10)$$

Where t_{ss} and t_{sr} are the sunset and sunrise hour, L_d accounts for the solar day length, and Δt_b is the interval at which the direct radiation strikes perpendicular to the surface.

To obtain collected daily energy, we use the expression:

$$\dot{\xi} = \bar{G}(r_d + r_b)S_{sph}L_d \quad (11)$$

Because the spherical surface does not intercept direct radiation perpendicular to the surface of the absorber over the same section [35], we must use spherical coordinates to calculate the effective absorbing surface, being:

$$S_{sph} = R^2\theta^2 = WH\theta^2 \quad (12)$$

Where W and H are the width and height of the absorption area, and R is the radius of the spherical solar collector.

Combining equations 9 to 12:

$$\dot{\xi} = \bar{G} \left(\frac{12}{\pi} \right)^2 WH\theta^4 L_d^2 \left[\frac{1}{\Delta t_b} + \frac{1}{(L_d - \frac{12}{\pi} \beta)} \right] \quad (13)$$

We can express the energy collected by a flat-plate collector by:

$$\dot{\xi} = \bar{G}WHL_d \quad (14)$$

Therefore:

$$\Delta \dot{\xi} = \bar{G}WHL_d \left\{ \left(\frac{12}{\pi} \theta \right)^2 \theta^2 L_d \left[\frac{1}{\Delta t_b} + \frac{1}{\left(L_d - \frac{12}{\pi} \beta \right)} \right] - 1 \right\} \quad (15)$$

We determine the solar day length from the equation:

$$L_d = \frac{2}{15} \cos^{-1}(-\tan \phi \tan \delta) \quad (16)$$

With:

$$\delta = 23.45 \sin \left(360 \frac{284 + n}{365} \right) \quad (17)$$

n is Julian day.

To reduce the amount of calculation, we use the representative day of every month to determine the declination (Table 1).

Table 1 Representative declination for every month of the year [31, 33].

Month	Day of the month	δ (°)
January	17	-20.9
February	16	-13.0
March	16	-2.4
April	15	9.4
May	15	18.8
June	11	23.1
July	17	21.2
August	16	13.5
September	15	2.2
October	15	-9.6
November	14	-18.9
December	10	-23.0

3. Description of the System

The prototype is a commercial spherical collector [36] of 1.05 m. in diameter, with an effective interception surface of 4.02 m² (Figure 1), whose selectivity is 19. Figure 2 shows a cutting view of the prototype.



Figure 1 View of the prototype.

A transparent plastic of high transmissivity ($\tau > 0.95$) covers the surface. The spherical surface absorbs not only direct solar radiation but diffuse one from both hemispheres, as well as reflected radiation from the ground. We measure the solar radiation onto a horizontal plane with an SKYE-TORN pyranometer [37], correcting the value for the appropriate angle using the expression:

$$G = G_o \cos\theta_z \tag{18}$$

Where:

$$\cos\theta_z = \sin\delta\sin\phi + \cos\delta\cos\phi\cos\omega \tag{19}$$

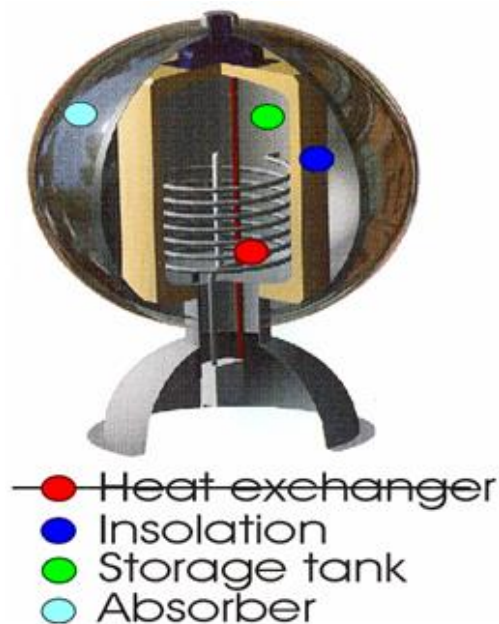


Figure 2 Cutting view of the prototype.

The tested flat-plate collector is a commercial unit [38] of 1.940 m in length and 1.025 m in width, with a surface of 1.989 m² (Figure 3). For the comparative analysis of an equal absorbing surface, we used two units for a global area of 3.997 m² that only differs by 1% from the spherical solar collector surface. For the comparative analysis of equal width and height, we used a single flat-plate collector with an opaque cover of 0.9 m length and 1.025 m width, resulting in an effective absorbing surface of 1.04 m × 1.025 m, which is very close to the diameter of the spherical solar collector.



Figure 3 View of the tested flat-plate collector.

To determine the received energy, we use a set of calibrated photocells of small size (5 mm × 5 mm) uniformly distributed onto the solar collector surface, and connected to an energy meter device that computes the signal from the photocell sensor and converts it into energy. The energy meter device operates with an accuracy of 0.1 W.

4. Simulation

In the first group of tests, we simulated the performance of the spherical and flat-plate collectors using equations 14 and 15, which gives the difference in collected energy from equation 16. We developed this group of tests in two sections, equal absorbing surface (test 1) and equal width and height (test 2).

For the simulation, we used the following values (Table 2):

Table 2 Data on the astronomical parameters.

Parameter	ϕ (°)	β (°)	γ (°)	ω (°)	δ (°)
Value	40.41	45	0	0	Depends on the day of the year

We consider a null solar angle value ($\omega = 0$) because we simulated the daily performance of the solar collector.

We use the typical meteorological year (TMY) to determine the solar radiation for the testing location. In our case (Figure 4):

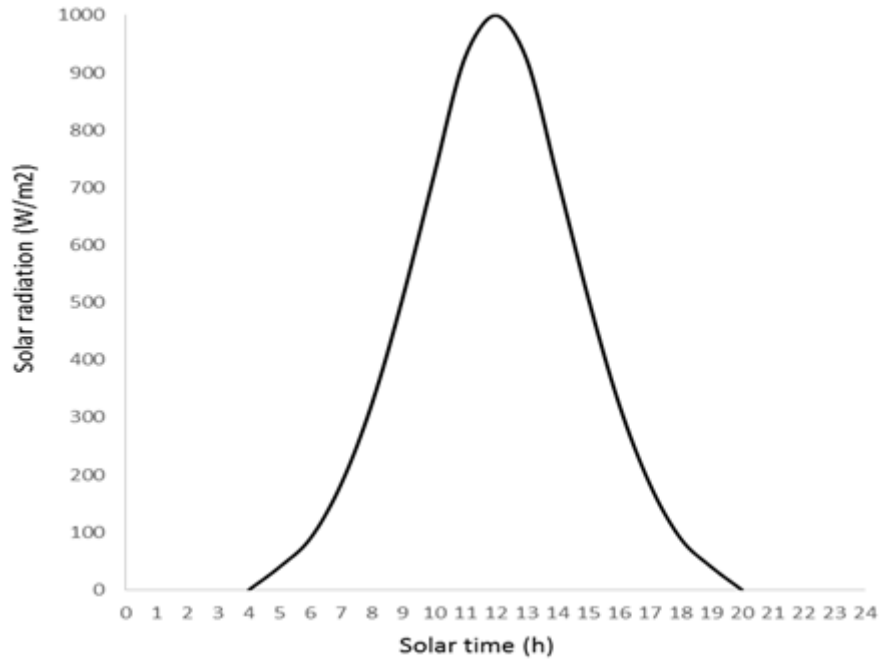


Figure 4 Daily distribution of solar radiation for the location of testing.

Applying equation 14, using values from Table 2 for the declination, and the dimensions of the double unit flat-plate collector, we have determined the amount of energy collected by a flat-plate and a spherical solar collector of the same absorbing area. The simulation calculates the collected energy for every solar time and cumulates the values for every day of the year, resulting in a global yearly contribution of the collected energy of 3775.5 kWh. Repeating the operation for the spherical solar collector and applying equation 13, we obtain a year contribution of 7892.8 kWh. Comparing both results, we realize the spherical solar collector generates more energy than the flat-plate one by a factor of 2.09. If we deal with the length and width of the flat-plate collector equal to the diameter of the spherical one, the global yearly contribution of the flat-plate collector reduces to 1021.7 kWh. Figure 5 shows the cumulative year energy distribution for the three cases. Flat-plate (covered) corresponds to the situation where we cover part of the collector to operate with the same width and height as the diameter of the spherical one.

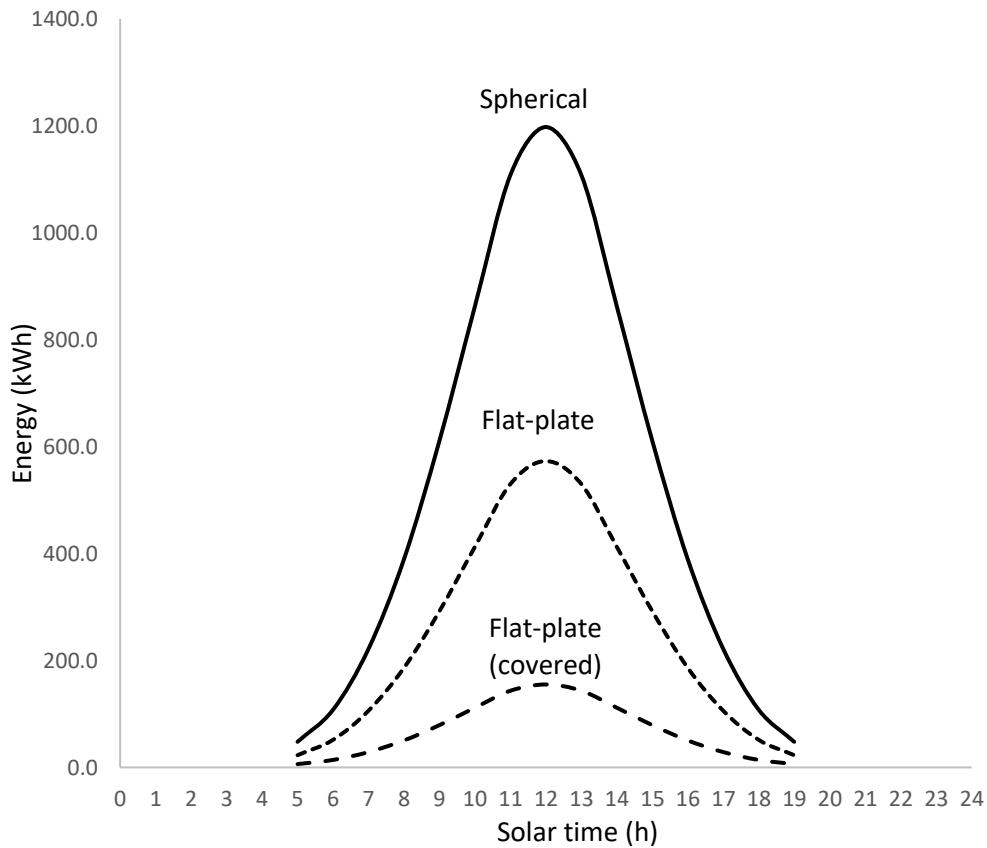


Figure 5 Cumulative year energy for the spherical and flat-plate collector at the everyday solar time.

Table 3 shows the ratio of the cumulative energy for the flat-plate collector compared to the spherical one.

Table 3 Ratio of cumulative yearly energy.

Solar collector type	Spherical	Flat-plate (equal absorbing surface)	Flat-plate (equal width and height)
Ratio	1.000	0.478	0.129

The analysis of the simulation results predicts that the use of spherical solar collectors increases the year collected energy from 209% for an equal absorbing area to 775% if case the width and height of the flat-plate collector equal the diameter of the spherical one.

5. Experimental Tests

To verify the validity of the simulation and the numerical results, we developed a group of experimental tests using the collectors described in section 3 and reproducing the simulation operating conditions. Figure 6 represents the results of the tests for the flat-plate collector with the same absorbing surface as the spherical one.

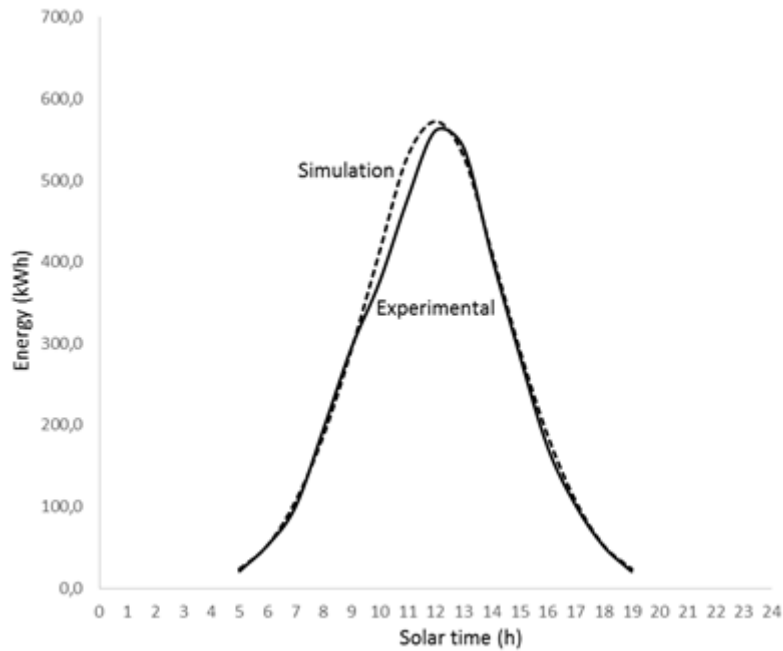


Figure 6 Cumulative year energy for the flat-plate collector at the everyday solar time (simulation and experimental).

Solar radiation is measured using a SKYE 1110 global radiation pyranometer of $\pm 0.1 \text{ W/m}^2$ resolution.

The accuracy in experimental measurements of collected energy is 0.1 Wh/m^2 .

The continuous line in Figure 6 represents experimental results, while the dashed line accounts for the simulation output data.

We observe a good correlation between experimental and simulation values, with a slight difference of 3.1% in the average daily collected energy.

Reproducing the test for the spherical and covered flat-plate collector, we obtain (Figure 7 and Figure 8):

As in the test of flat-plate collectors, there is a good correlation between experimental results and simulation data for the spherical solar collector. The adjustment coefficient of the subtended area for the two curves is 0.997.

As in Figure 6, the continuous line in Figure 7 and Figure 8 represents experimental results, while the dashed line accounts for the simulation output data.

The correlation between experimental results and simulation data is 0.970 for the case of the covered flat-plate collector.

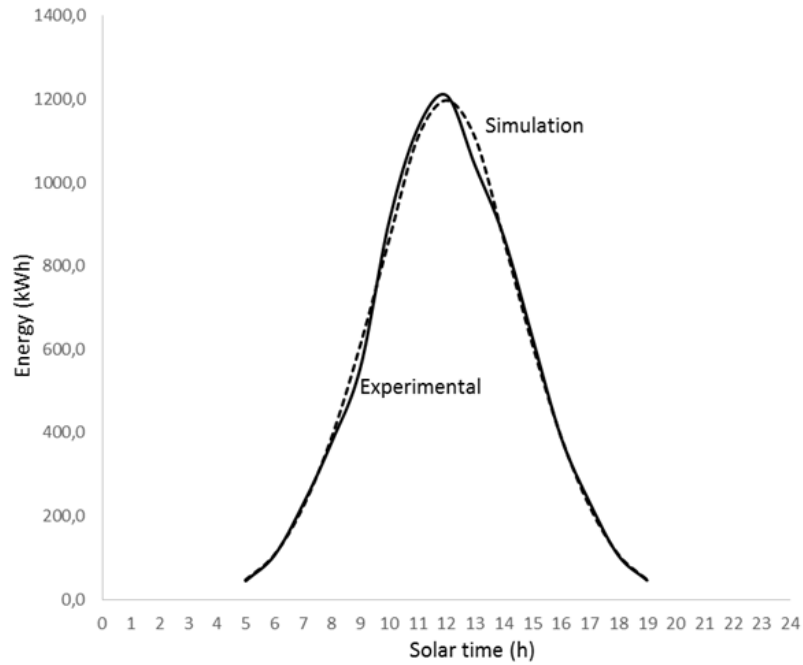


Figure 7 Cumulative yearly energy for the spherical collector at every day solar time (simulation and experimental).

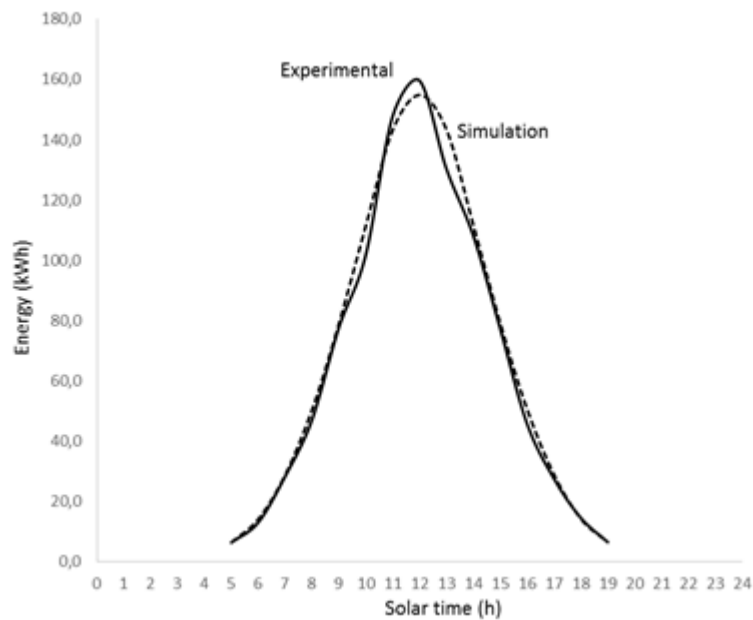


Figure 8 Cumulative yearly energy for the covered flat-plate collector at every day solar time (simulation and experimental).

The comparison between experimental results and simulation output data results in a good agreement, higher than 97% in the case of the flat-plate collector and close to 100% for the spherical one. Therefore, we consider the simulation procedure to be validated, and the prediction of collected solar energy is highly accurate.

Since the comparative analysis applies to general conditions, which include geometrical characteristics and dimensions of the spherical and flat-plate collectors, the developed study applies

to different types of solar collectors, spherical, semi-spherical, and flat-plate. Equations 13, 14, and 15 determine the collected energy and energy difference between two specific collectors, provided all geometric characteristics are known.

The study also applies to different regions and solar environmental conditions since the reference equations used in the calculations (equations 13.14 and 15) use the average global solar radiation on site, the angle of incidence, and the tilt of the solar collector.

6. Conclusions

The use of spherical solar collectors increases daily, monthly, and yearly collected energy. The average increase depends on the size of the collector.

For an equal absorbing surface, the spherical solar collector shows an increasing factor of 2.09 in the year average solar collected energy. For the case where the width and height of the flat-plate collector equal the diameter of the spherical one, the collecting energy by this latter one increases by a factor of 7.75.

The running of a simulation procedure based on the developed algorithms for the solar energy collection matches the results from experimental tests within 97% for the case of the flat-plate collector and 99.7% for the spherical one.

The validation of the simulation procedure allows us to predict the increase in solar energy collection when using spherical solar devices.

The study is valid for variable solar collectors' configurations and solar radiation conditions.

Author Contributions

The author did all the research work of this study.

Competing Interests

The author has declared that no competing interests exist.

References

1. Solanki A, Pal Y. Applications of a flat plate collector in dairy industries: A review. *Int J Ambient Energy*. 2022; 43: 1915-1923.
2. Mahdi K, Bellel N. Development of a spherical solar collector with a cylindrical receiver. *Energy Procedia*. 2014; 52: 438-448.
3. Bragado L. Study and characterization of a spherical solar collector [In Spanish]. Madrid: University of Madrid; 2011.
4. Gaspar F, Deac T, Tutunaru LV, Moldovanu D. Experimental study on the sun tracking ability of a spherical solar collector. *Energy Procedia*. 2016; 85: 220-227.
5. Elhefnawy MA, Ahmed AR, Awad MM. Experimental investigation on the performance of spherical solar collector for water heating. *Mansoura Eng J*. 2020; 41: 27-37.
6. Gaspar F, Balan M, Jantchi L, Ros V. Evaluation of global solar radiation received by a spherical solar collector. *Bull UASVM Agric*. 2012; 69: 128-135.
7. Klychev S, Bakhramov SA, Kharchenko V, Panchenko V. Research of heat losses of solar collectors and heat accumulators. *Int J Energy Optim Eng*. 2021; 10: 85-103.

8. Gulzar H, Tomar K, Malik Y. Solar energy collection using spherical sun power generation. *Int J Creat Res Thoughts*. 2021; 9: 60-65.
9. Samanta B, Al Balushi KR. Estimation of incident radiation on a novel spherical solar collector. *Renew Energ*. 1998; 14: 241-247.
10. Yari S, Safarzadeh H, Bahiraei M. Experimental study of an absorber coil in spherical solar collector with practical dimensions at different flow rates. *Renew Energy*. 2021; 180: 1248-1259.
11. Brock BC. *Optical analysis of spherical segment solar collectors*. Lubbock, Texas: Texas Tech University; 1977.
12. Sansoni P, Fontani D, Francini F, Jafrancesco D, Longobardi G. Optical design and development of fibre coupled compact solar collectors. *Light Res Technol*. 2007; 39: 17-30.
13. Ebaid MA, Salah SI, Abdel-Rehim AA. An experimental study of a hemi-spherical solar collector under Egyptian climate. *Case Stud Therm Eng*. 2021; 26: 101153.
14. Inalli M, Ünsal M, Tanyildizi V. A computational model of a domestic solar heating system with underground spherical thermal storage. *Energy*. 1997; 22: 1163-1172.
15. Pelēce I. Semi-spherical solar collector for water heating. *Proceedings of 9th International scientific conference "Engineering for rural development"*; 2010 May 27-28; Jelgava. Jelgava: LLU.
16. Pelece I, Ziemelis I. Water heating effectiveness of semi-spherical solar collector. *Proceeding of the International Scientific Conference of Renewable Energy and Energy Efficiency*; 2012 May 28-30; Jelgava, Latvia. Jelgava: Latvia University of Agriculture.
17. Cohen S, Grossman G. Development of a solar collector with a stationary spherical reflector/tracking absorber for industrial process heat. *Sol Energy*. 2016; 128: 31-40.
18. Yari S, Safarzadeh H, Bahiraei M. Experimental study of storage system of a solar water heater equipped with an innovative absorber spherical double-walled tank immersed in a phase change material. *J Energy Storage*. 2023; 61: 106782.
19. Suman S, Khan MK, Pathak M. Performance enhancement of solar collectors-A review. *Renew Sust Energy Rev*. 2015; 49: 192-210.
20. Armenta-Deu C. Performance test in semispherical solar collectors with discontinuous absorber. *Renew Energy*. 2019; 143: 950-957.
21. Pelēce I, Iljins U, Ziemelis I. Theoretical calculation of energy received by semi-spherical solar collector. *Agron Res*. 2008; 6: 263-269.
22. Pelece I, Ziemelis I, Iljins U. Surface temperature investigations of semi-spherical solar collector. *Biosyst Eng Environ*. 2009; 4: 370.
23. Tan Y, Zhao L, Bao J, Liu Q. Experimental investigation on heat loss of semi-spherical cavity receiver. *Energy Convers Manag*. 2014; 87: 576-583.
24. Yadav AS, Sharma SK. Numerical simulation of ribbed solar air heater. In: *Advances in Fluid and Thermal Engineering. Lecture Notes in Mechanical Engineering*. Singapore: Springer; 2021. pp. 549-558.
25. Yadav AS, Shukla OP, Bhadoria RS. Recent advances in modeling and simulation techniques used in analysis of solar air heater having ribs. *Mater Today*. 2022; 62: 1375-1382.
26. Prasad R, Yadav AS, Singh NK, Johari D. Heat transfer and friction characteristics of an artificially roughened solar air heater. In: *Advances in Fluid and Thermal Engineering. Lecture Notes in Mechanical Engineering*. Singapore: Springer; 2019. pp. 613-626.

27. Shrivastava V, Yadav A, Shrivastava N. Comparative study of the performance of double-pass and single-pass solar air heater with thermal storage. Proceedings of International Conference on Recent Advancements in Mechanical Engineering; 2020 July 8-9. Singapore: Springer Nature Singapore.
28. Yadav AS, Gattani A. Solar thermal air heater for sustainable development. Mater Today. 2022; 60: 80-86.
29. Schamer K, Greif J. The European solar radiation atlas vol. 1: Fundamentals and maps. Paris, France: Les Presses de l'Ecole des Mines; 2000.
30. Tian Z, Deng J, Zhang S, Yao R, Shao L. A quick measurement method for determining the incidence angle modifier of flat plate solar collectors using spectroradiometer. Sol Energy. 2020; 201: 746-750.
31. Duffie JA, Beckman WA. Solar engineering of thermal processes. Hoboken, NJ: John Wiley & Sons; 2013.
32. Sen Z. Solar energy fundamentals and modeling techniques: Atmosphere, environment, climate change and renewable energy. London: Springer; 2008.
33. Iqbal M. An introduction to solar radiation. Cambridge: Academic Press; 1983.
34. Tiwari GN, Tiwari A. Handbook of solar energy. Singapore: Springer; 2016.
35. Bakir Ö. Experimental investigation of a spherical solar collector. Çankaya, Turkey: Middle East Technical University; 2006.
36. Sfera Solar. ART ibérica SL (coming somewhen). Available from: www.artysol.com.
37. SP1110 Pyranometer Sensor. Campbell Scientific Ltd. Campbell Park, 80 Hathern Road, Shepshed, Leicestershire, LE 12 9RP, UK. Available from: www.campbellsci.co.uk.
38. Solar Water Heater, Model 180J, Solahart Industries Pty Ltd. 112 Pilbara Street, Welshpool, Western Australia 6106. Available from: www.solahart.com.au.